

# Shaping Art with Art: Morphological Analysis for Investigating Artistic Reproductions

Antonio Monroy<sup>1</sup>, Peter Bell<sup>1,2</sup>, and Björn Ommer<sup>1</sup>

<sup>1</sup> Interdisciplinary Center for Scientific Computing

<sup>2</sup> Institute of European Art History

University of Heidelberg, Germany

{antonio.monroy,pbell,bjoern.ommer}@iwr.uni-heidelberg.de

**Abstract.** Whereas one part of art history is a history of inventions, the other part is a history of transfer, of variations and copies. Art history wants to understand the differences between these, in order to learn about artistic choices and stylistic variations. In this paper we develop a method that can detect variations between artworks and their reproductions, in particular deformations in shape. Specifically, we present a novel algorithm which automatically finds regions which share the same transformation between original and its reproduction. We do this by minimizing an energy function which measures the distortion between local transformations of the shape. Thereby, the grouping and registration problem are addressed jointly and model complexity is obtained using a stability analysis. Moreover, our method allows art historians to evaluate the exactness of a copy by identifying which contours were considered relevant to copy. The proposed shape-based approach thus helps to investigate art through the art of reproduction.

## 1 Introduction

Computer vision and art history share the interest in similarity and shape. Cultural heritage consists not only of unique artworks but also of related reproductions. Art history wants to understand the differences between them in order to learn about artistic choices and stylistic variations. At the latest since Erwin Panofsky's book [1] about the Renaissance, we know how productive the inspiration of ancient art is. Works like the Apollo Belvedere or the Laocoön group inspired artists in the whole early modern period. But even accurate copies are labeled with stylistic signs of their present. To discover these differences, computer vision methods can be very helpful to bring new insights into the problem. Furthermore, European Art of the Middle Ages and early modern period is mainly reproduced in black and white prints or monochrome drawings which are also used to prepare paintings, sculptures, architecture or tapestries. Thus, color and appearance often only have brief occurrence on the timeline of an idea and its transformations. Therefore it seems justifiable to concentrate on shape when analyzing the reproduction processes.

Shape is also of enormous importance in computer vision as it is a key characteristic of objects and, as such, an important characteristic when detecting

or matching objects. Finding related structures, grouping affiliated fragments of shape, and characterizing the deformation of their Gestalt are therefore key problems in machine vision ([2]). Thus, shape analysis is a field, where art history and computer science can benefit from each other. Specifically, we develop a method which detects variations between artworks and their reproductions, while detecting groups that have been modified similarly and estimating their deformation. Consequently, we need to tackle two interrelated problems jointly: grouping regions of a scene that have been modified similarly and finding the transformations for those regions. These problems are addressed together by minimizing an energy function which measures the distortion between local transformations of the shape. The model complexity, i.e. the optimal number of groups is automatically determined based on a stability analysis of the scene transformation. Moreover, our method allows art historians to evaluate the exactness of a copy by identifying which contours were considered relevant to reproduce.

Subsequently, we discuss our approach in particular on several prominent reproductions based on hand drawings: the self-copying of the Ludwig Henfflins workshop in a medieval manuscript (*Story of Sigenot*, University of Heidelberg, cpg 67); reproductions of the Codex Manesse (University of Heidelberg, cpg 848), and lithographies of Johann Anton Ramboux after traced Italian paintings.

## 2 Related Work

In [3] the authors analyze the temporal drawing process of how an image is reproduced, assuming that parts drawn in closed succession in the reproduction exhibit similar transformations between them. Contrary to our approach, the authors of [3] needed to manually locate and match landmark points, since they did not provide an automatic contour extraction and matching procedure. The second limitation is the application of two different clustering algorithms. The first one groups points along the shape in order to estimate parameters of local affine transformations and assumes perfect correspondences between shapes. In a second step they apply a hierarchical clustering algorithm to further group points which share similar transformations. To find regions with similar affine transformations we formulate a single optimization problem, where affine transformations are estimated and points are grouped within the same procedure.

In the field of sparse motion segmentation, [4] presented a method for decomposing videos into similarly moving layers. The scene is firstly divided into a regular grid and an affine transformation is calculated for each block. This method estimates affine motion models for segments on a regular grid. Due to clutter and missing contours, accurate estimation of small and continuous deviations in transformations can not be estimated with this approach. In a similar way, [5] embed each shape in a lattice consisting of several connected squares and register them by estimating a rigid transformation for every square. Since the registration is only on the level of rigid squares, a grouping into flexibly shaped regions with related modifications is not part of this contribution. Furthermore, [5] is not able to handle deformations which do not preserve local rigidity (e.g. s scaling

or shear) and it requires a significant overlap between shapes for registration. Additionally, in our setting, background clutter creates distractors that need to be handled, whereas the method of [5] is only applied to cartoons without any clutter. Whereas [6] tries to ensure consistent perspective in art images, [7] is concerned with images that feature convex mirrors and presents an algorithm for dewarping image reflections on those mirrors.

### 3 Approach

Our algorithm automatically detects subtle variations between unique artworks and their reproductions that can even elude trained eyes, especially when detailed scenes or large quantities of image material are to be judged. The goal is not to supplant, but to enhance connoisseurship. For this we need to bring both images into correspondence and reason about the morphological deformation and alteration between both. Due to deliberate alterations or due to geometrical errors accumulated during the drawing process, different parts in an image are transformed differently. A typical example for a deliberate alteration is the movement of an articulated part between the original and its reproduction. The second class of deformations is more subtle and is related to the drawing process. Copying in many cases worked by placing a thin, tracing paper on top of the original, and sketching the contours. Movements of the semi-opaque sheet by the artist induced slight modifications in the reproduction. Whereas parts which were reproduced at the same time share the same transformation, sheet movements induced a different transformation for the rest of the reproduction. For both types of deformation we model the complex overall distortion during reproduction by finding the different image parts which share similar transformations and then applying this transformation to the corresponding image regions. Our algorithm is fully automatic and it finds the regions in the original image which similarly transform between both images and simultaneously obtains the different local transformations. Moreover, the approach allows us to measure the similarity between transformations giving us a deeper understanding of the present modifications.

Finally, using our model we are able to infer which contours were considered relevant by the artist (see Sec. 3.3) for the reproduction of the image. This capability is an important step in the process of learning about specific choices of an artist or a specific art school for the reproduction of images.

#### 3.1 Bringing images into correspondence

For a long time there has been a predominant emphasis on contours and shape in European Art since the Middle Ages and early modern period. An example is Johann Anton Ramboux (1790-1860) who was part of the the Nazarenes movement. This German group of artists admired medieval art up to Raphael especially works where a strict line drawing outplays colors and textures. Contours he traced from original images were assumptions for the position of the



**Fig. 1.** Cartoon sequence. (a) 1st (blue) and 4th (red) frame. (b) Groups found by our algorithm of Sec. 3.2. (c) TPS interpolation with artefacts enclosed in a circle (e) Our piecewise affine transformation using the found groups.

shapes in the original painting.

Similarly, contours have played an important role in the analysis of shape, growth, deformation and movement within computer science ([2]). The underlying idea for the development of many state-of-the-art analysis tools has been the observation that shape communicates itself through contours. To describe a shape we extract the underlying contours and then locate a discrete number of landmark points, on the contours of the object. We then match both point-sets and use a piecewise affine transformation model to transform all contours (and not only the landmark-points) present in the image.

**Contour extraction.** Depending on the drawing technique, different methods for contour extraction need to be used. For contour-based shape drawings we have to deal with different contour thickness and texture. Hence, we first extract the contours by convolving the image with different Laplace of Gaussian (LoG) Filters of varying sigmas ( $\sigma = 0.8 + j * 0.4$ ,  $j = 1, \dots, 9$ ) and then take the maximal response over all sigmas for every pixel. This kind of filter is suitable since it allows to obtain a single response for lines of varying thickness and ensure in praxis a good contrast between ridge response and background. Finally, non-maximum suppression followed by hysteresis thresholding is applied to obtain a single binary response. Landmark points for a shape representation are then uniformly sampled along the contours. For the second kind of images, where shape is encoded through texture and color boundaries we use the Pb code ([8]) for edge extraction, which weight the edge signal proportionally to their strength. By setting a high threshold on the output, we discard most of the noise in the edge signal at the cost of losing relevant shape details. In Sec. 3.3 we describe how to separate shape information from noise, using a replica of the image.

A point set representing a shape in the original image is referred to with  $Y := \{y_i \in \mathbb{R}^{3 \times 1}\}_i^n$  and with  $X := \{x_i\}_i^m$  in the reproduction. Both point-sets are given in homogeneous coordinates.

### 3.2 Finding groups of transformations

In this section we assume to have the correspondence between  $X$  and  $Y$  (described in the next Sec.) and we solve our main task: to find those groups in

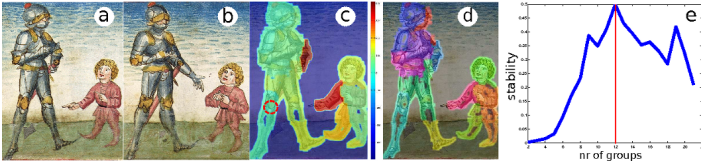


**Fig. 2.** (a)(b) Ludwig Henfflins workshop, *Story of Sigenot*, cpg. 67 (c) Distances between transformations w.r.t the red circle (d) 12 groups of deformation (e) Stability analysis to automatically select the number of groups.

the image which share the same transformation at the same time that the transformations are estimated. These groups correspond to image regions which are reproduced similarly by the artist. Each of these groups is modeled through an affine transformation capable of transforming the group from the reproduction into the original painting. Hence, the problem consists in estimating a binary data assignment matrix  $M \in \mathbb{B}^{n \times k}$  of  $n$  points to  $k$  groups at the same time as we calculate different affine transformations  $T^\nu \in \mathbb{R}^{3 \times 3}$  ( $\nu = 1, \dots, k$ ) for each group. For the matrix  $M$  we have  $m_{i\nu} = 1$  only if point  $\mathbf{x}_i$  is assigned to group  $\nu$ . At the same time,  $T^\nu$  registers all points for which  $m_{i\nu} = 1$ . Finding  $M$  and  $T^\nu$  is difficult since both terms are mutually dependent. On the one side, we need the assignment matrix  $M$  in order to calculate  $T^\nu$ . On the other side we need  $T^\nu$  to infer the points  $\mathbf{x}_i$  belong to the group  $\nu$ . We observe that calculating the optical flow and clustering the resulting vector fields features only insufficient accuracy: contours have been distorted (e.g. stretched), junctions are partly missing and textures alongside the contours have not been reproduced.

To find both,  $M$  and the affine transformations  $T^\nu$ , we first calculate local affine transformations  $T_i$ . These transformations are different from  $T^\nu$ . While the former are calculated using only a small neighborhood around each landmark point (12 non-collinear points) and are kept fix, the latter transformations of groups  $T^\nu$  correspond to the deformations present in the reproduction process and are optimized together with  $M$ . We then define an energy function  $E(M, T^\nu)$ , which we minimize using coordinate descent and deterministic annealing. The overall energy function we seek to optimize is:

$$\min_{M, T^\nu} E(M, T^\nu) = \min_{M, T^\nu} \frac{1}{2} \sum_{\nu=1}^k \sum_{i=1}^n \sum_{j=1}^n \frac{M_{i\nu} M_{j\nu}}{p_\nu} a_{ij} + \sum_{\nu=1}^k \sum_{i=1}^n M_{i\nu} r_{i\nu} \quad (1)$$

$$s.t. \quad \sum_{\nu=1}^k M_{i\nu} = 1 \quad (\forall i = 1, \dots, n), \quad M_{i\nu} \in \{0, 1\} \quad (2)$$

$$a_{ij} := \frac{1}{Z} (\|T_j x_i - T_i x_i\| + \|T_j x_j - T_i x_j\|) \quad (3)$$

$$r_{i\nu} := \frac{1}{Z_i} (\lambda_2 \|T^\nu x_i - y_i\|_2^2 + (1 - \lambda_2) \|T_i x_i - T^\nu x_i\|_2^2), \quad (4)$$

where  $Z_i := \sum_{\nu=1}^k r_{i\nu}$ ,  $Z := \max a_{ij}$  and  $p_\nu := \sum_{i=1}^n M_{i\nu}/n$  are normalization constants and  $a_{ij}$  measures the pairwise distortion between local transformations  $T_i$  and  $T_j$ ;  $r_{i\nu}$  describes the cost of assigning point  $i$  to group  $\nu$  and consists of two weighted terms. The first one measures how well a point  $x_i$  can

be registered against  $y_i$  and the second term forces the local transformation  $T_i$  (corresponding to point  $x_i$ ) to be similar to the group transformation  $T^\nu$ . We use  $\lambda_2 = 0.8$  to control the tradeoff between both terms. Finally, in (1),  $p_\nu$  normalizes clusters by their size. In our case, we allow points to belong to a single group. Thus, we additionally obtain the constraint  $\sum_{\nu=1}^k M_{i\nu} = 1$ . We first describe how to iteratively update the matrix  $M$ . The basic idea is to relax it to be a continuous valued matrix  $\hat{M}$  in the interval of  $[0, 1]$  and introduce a  $M \log M$  entropy barrier function, which allows fuzzy, partial assignments of data points to groups in the matrix  $\hat{M}$ . This term is controlled by a temperature parameter  $\beta$ . For  $\beta \rightarrow 0$  we obtain a minimum of the discrete energy  $E(M, T^\nu)$ . The relaxed energy function  $\hat{E}(\hat{M}, T^\nu; \beta)$  is defined as follows

$$\min_{\hat{M}, T^\nu} \hat{E}(\hat{M}, T^\nu; \beta) := \frac{1}{2} \sum_{\nu=1}^k \sum_{i=1}^n \sum_{j=1}^n \frac{\hat{M}_{i\nu} \hat{M}_{j\nu}}{p_\nu} a_{ij} + \sum_{\nu=1}^k \sum_{i=1}^n \hat{M}_{i\nu} r_{i\nu} \quad (5)$$

$$+ \beta \sum_{\nu=1}^k \sum_{i=1}^n \hat{M}_{i\nu} (\log \hat{M}_{i\nu} - 1) \quad (6)$$

$$s.t. \quad \sum_{\nu=1}^k \hat{M}_{i\nu} = 1 \quad (\forall i = 1, \dots, n), \quad \hat{M}_{i\nu} \in \{0, 1\} \quad (7)$$

As described in [9], the minima of  $E(M, T^\nu)$  and  $E(\hat{M}, T^\nu; \beta)$  all coincide in the limit  $\beta \rightarrow 0$  if the matrix  $(a_{ij})$  is negative definite. This can be obtained by adding a sufficiently large term to its diagonal without altering the structure of the minima of  $E(M, T^\nu)$ . The linear constraints are imposed by adding a Lagrange multiplier term obtaining the Lagrange function

$$L(\hat{M}, \mu) := \frac{1}{2} \sum_{\nu=1}^k \sum_{i=1}^n \sum_{j=1}^n \frac{\hat{M}_{i\nu} \hat{M}_{j\nu}}{p_\nu} a_{ij} + \sum_{\nu=1}^k \sum_{i=1}^n \hat{M}_{i\nu} r_{i\nu} \quad (8)$$

$$+ \beta \sum_{\nu=1}^k \sum_{i=1}^n \hat{M}_{i\nu} (\log \hat{M}_{i\nu} - 1) + \sum_{i=1}^n \mu_i \left( \sum_{\nu=1}^k \hat{M}_{i\nu} - 1 \right) \quad (9)$$

The Lagrangian function is a sum of a convex function  $E_{\text{vex}}(\hat{M}) = \beta \sum_{\nu i} \hat{M}_{i\nu} \log \hat{M}_{i\nu}$  and a concave part  $E_{\text{cave}}(\hat{M}) = (1/2) \sum_{\nu ij} \frac{\hat{M}_{i\nu} \hat{M}_{j\nu}}{p_\nu} a_{ij} + \sum_{\nu i} \hat{M}_{i\nu} r_{i\nu}$ . Using this fact, we can use the CCCP algorithm ([10]), which guarantees the minimization of the energy using the following update rule

$$\beta \left( 1 + \log \hat{M}_{i\nu}^{t+1} \right) = -\frac{1}{2} \sum_j \hat{M}_{j\nu}^t \frac{a_{ij}}{p_\nu} - r_{i\nu}. \quad (10)$$

After setting to zero the derivative of (8) with respect to  $\mu_i$ . We substitute it into equation (10) and solve for  $\hat{M}_{i\nu}^{t+1}$  and obtain

$$\hat{M}_{i\nu}^{t+1} = \frac{\exp \left( \beta \left( -\frac{1}{2} \sum_j \hat{M}_{j\nu}^t \frac{a_{ij}}{p_\nu} - r_{i\nu} - 1 \right) \right)}{\sum_\nu \exp \left( \beta \left( -\frac{1}{2} \sum_j \hat{M}_{j\nu}^t \frac{a_{ij}}{p_\nu} - r_{i\nu} \right) \right)} \quad (11)$$



**Fig. 3.** (a) Johann Anton Ramboux reproduction of (c) Pietro Perugino, *Assumption of the Virgin with four Saints*, 1500 (b) Noise-free contours of the Ramboux reproduction (a) using LoG filters (d) Binary Pb edge-signal of the Perugino (e) Relevant contours of the painting that match to contours of the reproduction. Hence, noisy edges of (d) are suppressed

After each update step (11), we recalculate the affine transformations using the Levenberg-Marquardt algorithm:

$$T^\nu = \arg \min_{T^*} = \sum_i^N \hat{M}_{i\nu}^{\dagger+1} (\lambda_2 \|T^* x_i - y_i\|^2 + (1 - \lambda_2) \|T_i x_i - T^* x_i\|_2^2) \quad (12)$$

To initialize the matrix  $\hat{M}^0$  we run a fuzzy c-means algorithm using the Euclidean distance between points  $x_i$  ([11]) and  $\hat{M}^0$  are the resulting fuzzy assignments. We use fuzzy c-means since it naturally provides us with probability assignments, which we require at a high temperature. Although a global minimum cannot be guaranteed, we observed good results using this optimization.

**Stability Analysis.** We estimate model complexity (i.e., the optimal number of clusters) using a stability analysis. For a number of clusters  $k$ , we randomly sample a subset of the points in  $X$  and run our algorithm  $b_{max}$  times on this subset, obtaining  $C_b$  clustering results. We first measure the distance between two clustering results using the minimal matching distance ([12])  $d(C, C') = \min_{\pi} \frac{1}{N} \sum_{i=1}^N \mathbb{1}_{[C(i) \neq \pi(C'(i))]}$ , where the minimum is taken over all permutations  $\pi$  of the  $k$  labels. The stability for a given  $k$  is then defined as the normalized mean  $stab(k) := \frac{1}{Z(k)} \left( 1 - \frac{1}{b_{max}^2} \sum_{b,b'} d(C_b, C_{b'}) \right)$ . In our experiments we have observed that the normalization  $Z(k) = 1 + \exp(-(k-8))$  favorably compensates the bias of stability analysis towards few clusters.

**Correspondence between landmark points.** To obtain correspondences between  $X$  and  $Y$  we automatically match both sets using [13]. This algorithm alternates between the calculation of correspondences and a non-parametric regularized displacement field between both point sets. This transformation model is defined only on the discrete set of points and it cannot be extended for the rest of the contours in the image. Hence, we require to use our piecewise affine transformation model for registration of the entire scene.

### 3.3 Discovering relevant strokes

Using an example (Fig. 3 (c) a detail of Pietro Perugino (c. 1445/1450-1523), *the Assumption of the Virgin with four Saints*) we describe now a method of how to discover which details are considered relevant by an artist during the reproduction. In (a) we have the contour-based reproduction from Ramboux. Which details of the painting are being reproduced? and which of them are neglected? We are interested in determining which contours in the painting are copied. Figure 3 (d) shows the unthresholded Pb edge-output of the Perugino. A very low signal-to-noise ratio on the output is very common on these kind of images. Our method suppresses the noise in order to obtain the contours in the painting which are also present in the reproduction. For this, we calculate the distance transform image of the registered Ramboux and then multiply the noisy edge map of the original image with this distance transform. This is equivalent to weight each edge pixel in the painting (including the noise) with the distance to the nearest Ramboux edge signal. Thus, the pixels which are also present in the Ramboux obtain a high score, whereas edge pixels resulting from noise are downweighted. In Figure 3 (e) we retain only the contours of the painting which have been distorted less than 3 pixels in the Ramboux (after correcting for the overall affine transformation).

## 4 Results

**Synthetic data.** A hand drawn cartoon sequence is used. It consists of 20 frames and illustrates a running horse with some kids on the back. Fig. 1 (a) shows the drawing of frames 1 in blue and 4 in red color. Several deformations between frames occur. Our algorithm correctly finds the parts in the image and manifests our perception of the articulated movement (Fig. 1 (b), different colors indicate different groups). Each group is associated with an affine transformation. Additionally, given the correspondences between frame 1 and 4, we applied a Thin Plate Spline (TPS) to register both frames (c). Using different weights for the regularization term we always observed transformation artefacts with the TPS (enclosed in a circle), and significant distortions to the structure of the image, which is undesirable for art comparison. In (d) we see that our piecewise transformation model alliviates this problem.

**Ancient Reproductions.** In contrast to our other examples where the reproductions were made hundreds of years after the creation of the original, the illuminator in Ludwig Henfflins workshop in c. 1470 loosely traced copies from scenes he had previously drawn himself. The *Story of Sigenot* (cpg. 67) shows very similar images. Like in a flip-book, the draftsman changes only parts of the illustration. This efficient method got possible with the substitution of parchment by a more transparent paper.

In Fig. 2 and Fig. 4 (b) we evaluate the performance of our algorithm on two examples of cpg. 67. The fourth thumbnail presents the groups found (using 4K landmarks for the whole scene) by our algorithm. We correctly recover the most relevant changes in the image (e.g. arm and feet movements). The third



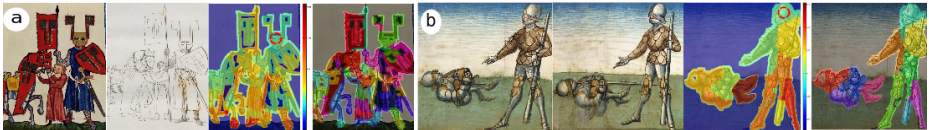


**Fig. 4.** (a) *Wolfram von Eschenbach*, Codex Manesse and Franz Hegi (1809/10) reproduction (b) *Story of Sigenot*, University of Heidelberg, cpg. 67

thumbnail shows the dissimilarity between the different transformations (measured w.r.t. the group with a red circle). Here,  $\|\log(T^i) - \log(T^j)\|_F$  is used to measure the distance between affine transformations. The analysis of these transformations reveals details about the copying process. Like in a normal drawing process, we see semantically relevant groups: the head, face, torso and extremities. Contrary to this, we show an example in Fig. 4 (a), which requires a very high number of groups (41) for registration and features high differences between transformations. This shows that the reproduction from Franz Hegi was sketched freehand after the Codex Manesse as opposed to Henfflin’s workshop.

Further comparisons against [3], which we cannot include due to space restrictions, also showed comparable groupings although our approach is fully automatic and does not require manual placement and registration of points.

**Stability Analysis.** We use 60% of the points in  $X$  for subsampling and set  $b_{max} = 10$  (sec. 3.2). In Fig. 2 (e) we plot the stability of our algorithm as a function of the number of clusters. In this case, we see that maximal stability is obtained for 12 groups (c). Choosing less groups would result in a poor registration, whereas increasing the number, would result in clusters sensible to noise.

**Discovering relevant strokes.** In section 3.3 we described a method for discovering which contours were relevant for an image reproduction and Fig. 5 shows further experiments on different reproductions. In (a) we register the reproduction (white contours) to the original painting. (b) shows the binary edge-signal and (c) presents the weighting of (b) using our method described in Sec. 3.3. Using our method we see how close Ramboux kept to the original. This has a further value for reconstructing the shape of originals that are partially lost. Furthermore, this method provide art historians with precise detail information about the style and attitude of the Nazarenes.

## 5 Conclusion

The analysis shows that related artworks, especially originals and their pre- or reproduced line drawings help to find contours in complex paintings. The comparison indicates that even the tracing process, which seems to be a relatively precise method, shows different transformations. They result from the moving and reattached tracing paper and further alterations. The grouping of the deformations reveals details about the process of copying. Like in a normal drawing process, the task is divided in different sections: the head, face, torso and ex-

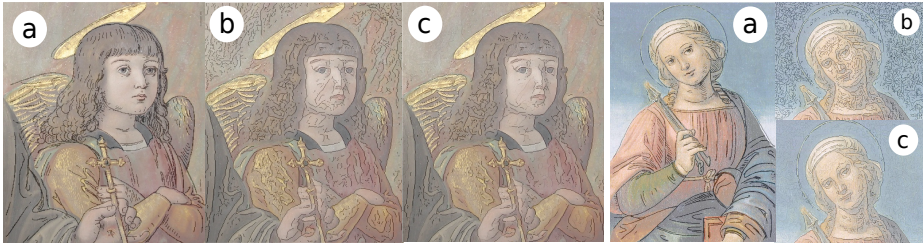


**Fig. 5.** (a) Registration of painting detail with Ramboux contour-based reproduction (black lines). (b) noisy edge-signal [9] of original painting (black lines) (c) registration-based weighting of edge-signals from (b) (Sec. 3.3).

tremities. Whereas the medieval illuminations provide very few, clear contours, J. A. Ramboux sometimes had to decide whether to treat a line as a contour or neglect it.

**Acknowledgements.** This work was supported by the Excellence Initiative of the German Federal Government, DFG project number ZUK 49/1

## References

1. Panofsky, E.: Renaissance and Resurrections in Western Art. Harper (1960)
2. Dryden, I.L., Mardia, K.V.: Statistical Shape Analysis. Wiley (1998)
3. Monroy, A., Carque, B., Ommer, B.: Reconstructing the drawing process of reproductions from medieval images. In: ICIP. (2011)
4. Wang, J., Adelson, E.: Representing moving images with layers. IEEE Trans. on IP **3**(5) (1994)
5. Sýkora, D., Dingliana, J., Collins, S.: As-rigid-as-possible image registration for hand-drawn cartoon. In: NPAR. (2009)
6. Chang, Y.S., Stork, D.G.: Warping realist art to ensure consistent perspective: A new software tool for art investigations. In: Human vision and electronic imaging. (2012)
7. Usami, Y., Stork, D.G., Fujiki, J., Hino, H., Akaho, S., Murata, N.: Improved methods for dewarping images in convex mirrors in fine art: Applications to van Eyck and Parmigianino. In: Computer vision and Image analysis of art II. (2011)
8. Maire, M., Arbelaez, P., Fowlkes, C., Malik, J.: Using contours to detect and localize junctions in natural images. In: CVPR. (2008)
9. Yuille, A., Kosowsky, J.: Statistical physics algorithms that converge. Neural Computation (6) (1994) 341–356
10. Yuille, A., Rangarajan, A.: The concave-convex procedure (cccp). In: Advances in Neural Information Processing Systems 14. (2002)
11. Bezdek, J.: Pattern Recognition with fuzzy objective function algorithms. Plenum Press (1981)
12. v. Luxburg, U.: Clustering stability: an overview. Foundations and Trends in Machine Learning **2**(3) (2010)
13. Myronenko, A., Song, X.: Point set registration: coherent point drift. PAMI **32**(12) (2010)